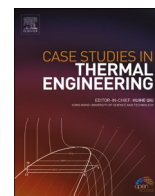




ELSEVIER

Contents lists available at ScienceDirect

## Case Studies in Thermal Engineering

journal homepage: [www.elsevier.com/locate/csite](http://www.elsevier.com/locate/csite)

# Investigating the effect of the number of layers of the atomic channel wall on Brownian displacement, thermophoresis, and thermal behavior of graphene/water nanofluid by molecular dynamics simulation

Xinwei Guo<sup>a,b,l,\*\*</sup>, Dheyaa J. Jasim<sup>c</sup>, As'ad Alizadeh<sup>d,\*\*\*</sup>, Babak Keivani<sup>e</sup>,  
Navid Nasajpour-Esfahani<sup>f</sup>, Soheil Salahshour<sup>g,h,i</sup>, Mahmoud Shamsborhan<sup>j</sup>,  
Rozbeh Sabetvand<sup>k,\*</sup>

<sup>a</sup> Ural Institute, North China University of Water Resource and Electric Power, Zhengzhou, Henan, 450045, China

<sup>b</sup> Institute of Thermal Energy Engineering, School of Mechanical Engineering, Shanghai Jiao Tong University, Shanghai, 200240, China

<sup>c</sup> Department of Petroleum Engineering, Al-Amarah University College, Maysan, Iraq

<sup>d</sup> Department of Civil Engineering, College of Engineering, Cihan University-Erbil, Erbil, Iraq

<sup>e</sup> Kırşehir Ahi Evran University, Department of Mechanical Engineering, 40200, Merkez, Kırşehir, Turkey

<sup>f</sup> Department of Material Science and Engineering, Georgia Institute of Technology, Atlanta, 30332, USA

<sup>g</sup> Faculty of Engineering and Natural Sciences, Istanbul Okan University, Istanbul, Turkey

<sup>h</sup> Faculty of Engineering and Natural Sciences, Bahcesehir University, Istanbul, Turkey

<sup>i</sup> Department of Computer Science and Mathematics, Lebanese American University, Beirut, Lebanon

<sup>j</sup> Department of Mechanical Engineering, College of Engineering, University of Zakho, Zakho, Iraq

<sup>k</sup> Department of Energy Engineering and Physics, Faculty of Condensed Matter Physics, Amirkabir University of Technology, Tehran, Iran

<sup>l</sup> Xi'an University of Science and Technology, State Key Laboratory of Green and Low-carbon Development of Tar-rich Coal in Western China, Xi'an, Shaanxi 710054, China

## ARTICLE INFO

Handling Editor: Huihe Qiu

## Keywords:

Brownian displacement

Thermophoresis

Thermal behavior

Molecular dynamics simulation

Graphene/ water nanofluid

## ABSTRACT

Nanofluids (NFs) are nanoscale colloidal suspensions containing dense nanomaterials. They are two-phase systems with solid in liquid phase. Due to their high thermal conductivity, nanoparticles increase the thermal conductivity (TC) of base fluids, one of the basic heat transfer parameters, when distributed in the base fluids. The present research investigates the thermal behavior, Brownian motion, and thermophoresis of water/graphene NF affected by different numbers of atomic wall layers (4, 5, 6 and 7) by molecular dynamics (MD) simulation. This investigation reports changes in heat flux (HF), TC, average Brownian displacement, and thermophoresis displacement. By raising the number of atomic wall layers from 4 to 7, the average Brownian displacement and thermophoresis displacement increase from 3.06 Å and 23.88 Å to 3.62 and 25.05 Å, respectively. Increasing the number of layers due to the decrease in temperature increases the temperature difference between the hot and cold points along the channel. It increases the Brownian motion and the maximum temperature. Additionally, by raising the atomic layers of the channel wall, the values of HF and TC increase from 39.54 W/m<sup>2</sup> and 0.36 W/mK to 41.18 W/m<sup>2</sup> and 0.42 W/mK after 10 ns, respectively. The temperature rose from 1415

\* Corresponding author.

\*\* Corresponding author. Ural Institute, North China University of Water Resource and Electric Power, Zhengzhou, Henan, 450045, China.

\*\*\* Corresponding author.

E-mail addresses: [gxxwos@126.com](mailto:gxxwos@126.com) (X. Guo), [asad.alizadeh2010@gmail.com](mailto:asad.alizadeh2010@gmail.com) (A. Alizadeh), [rozbeh.sabetvand@iaukhsh.ac.ir](mailto:rozbeh.sabetvand@iaukhsh.ac.ir) (R. Sabetvand).

<https://doi.org/10.1016/j.csite.2023.103859>

Received 10 September 2023; Received in revised form 25 November 2023; Accepted 2 December 2023

Available online 12 December 2023

2214-157X/© 2023 The Authors. Published by Elsevier Ltd. This is an open access article under the CC BY license (<http://creativecommons.org/licenses/by/4.0/>).

to 1538 K. These results are useful in different industries, especially for improving the thermal properties of different NFs.

### Abbreviations

NFs	Nanofluids
TC	Thermal conductivity
MD	Molecular Dynamics
HF	Heat flux
RDF	Radial distribution function
EAM	Embedded-Atom Method
LJ	Lennard-Jones
LAMMPS	large-scale atomic/molecular massively parallel simulation

### Nomenclature

$r_{ij}$	The distance between particles (m)
$u_i$	The potential of a particle (eV)
$\epsilon_{ij}$	Depth of the potential well (Kcal/mol)
$\sigma_{ij}$	Finite distance in which the potential is zero( $\text{\AA}$ )
$r$	The distance of the particles from each other
$U_{ij}$	The electric potential (eV)
$V$	The total volume of particles ( $\text{\AA}^3$ )
$k_B$	Boltzmann constant ( $1.380649 \times 10^{-23} \text{ J K}^{-1}$ )
$T$	The system temperature (K)
$J$	The heat flux( $\text{W/m}^2$ )
$m_i$	The mass of the particle(g)
$a_i$	The acceleration of the particle ( $\text{m}\cdot\text{s}^{-2}$ )
$N_{fs}$	The number of degrees of freedom
$F_\alpha$	Constant coefficient between 0 and 1
$\rho_\beta$	An attraction force caused by the presence of particles in the simulated box
$\varphi_\beta$	A repulsive force caused by atomic charge density

## 1. Introduction

Nanofluids are a new class of fluids engineered by dispersing nanometer-sized materials. To be more precise, NFs are nanoscale colloidal suspensions containing dense nanomaterials [1,2]. It is known that NFs have increased thermophysical properties such as TC, viscosity, and convective heat transfer coefficient [3]. Among the nanostructures used in NFs today, special attention is paid to graphene. Each graphene layer comprises hexagonal carbon rings that create a honeycomb structure [4]. In short, this structure is strong and thin, light, almost transparent, a very good thermal and electrical conductor, and has special electronic features [5]. Moreover, the movement of particles immersed in a fluid after colliding with fast atoms or molecules is called Brownian motion or random motion [6]. The reason why Brownian motion occurs is the application of force on particles. Many forces are applied to the particle in different directions [7]. Thermophoresis force is applied to the particles to decrease the temperature. It is caused by the increase in the movement of the molecules of the colliding fluid on the warmer side of the particle [8]. Due to the many advantages of NFs, especially their properties in heat transfer, NFs and factors affecting their behavior have been the subject of many researches, such as Sheikholeslami et al. [9] investigated the influence of uniform magnetic force on the thermal behavior of water-based NF in a porous container. The results indicate that the consideration of higher magnetic forces leads to a more conducive mechanism, and the permeability can increase the temperature gradient. Alilat et al. [10] investigated the influence of the cavity's inclination and aspect ratio on the behavior of a conical antenna cooled with NF-saturated porous media. It was concluded that the ratio of dimensions and slope of the cavity affects the thermal behavior of the active cone. Chattopadhyay et al. [11] simulated the magnetic mixed convective flow and the hybrid NF's thermal behavior in a partially heated wavy cavity. The simulations show a significant increase in thermal performance with increasing magnetic orientation, corrugation, and solid concentration of nanoparticles. Li et al. [12] studied the thermal behavior of pool boiling heat transfer of the water-based NF and the effect of the number of iron nanoparticles on it. Ruhani et al. [13] investigated the thermal characteristics of a new NF with cerium oxide powder. It was observed that with increasing of  $\varphi$  and temperature, the TC ratio of the NF increases. Zamen et al. [14] studied the application of  $\text{Al}_2\text{O}_3$ /water NF as a coolant in the new design of photovoltaic/thermal system. The obtained results show that adding nanoparticles to pure water can significantly increase the efficiency of the photovoltaic/thermal device. The researchers' results show that the channel type affects the flow and movement of atoms [15–19]. For example, Saeed et al. [20] investigated partial slip on double-diffusive convection on peristaltic waves of johnson–segelman NFs under the impact of inclined magnetic field. The results show that the slip effect in the channel causes the fluid

particles to stray, slowing the fluid velocity. Moreover, as thermophoretic effects and Brownian motion increase, nanoparticles rapidly move from the wall into the fluid, significantly raising the temperature. Akram et al. [21] investigated the peristaltic motion of an asymmetric channel carrying magneto-Prandtl NF under double-diffusive convection, including thermal and concentration gradients. The findings of this investigation can be beneficial in improving gastrointestinal movements and pumping in various engineering devices. Akram et al. [22] investigated the effect of magnetic field and double-diffusive convection on thermally radiative peristaltic flow of Prandtl tilted magneto NF in an asymmetric channel with effects of partial slip and viscous dissipation. The results show that as the Grashof number increases, the drag force decreases, increasing the axial velocity.

In line with the aforementioned statements, NFs with their many features and advantages, such as their features in heat transfer in various industries, have been studied by many researchers. Many of these researches have dealt with NFs from different perspectives. Also, some investigations have been done using the MD simulation [23–25]. In a recent essay, the influence of layers 4, 5, 6, and 7 on graphene-water NF's atomic and thermal behavior was investigated using MD simulation. For this investigation, the thermal behavior of the samples, temperature profile, HF, TC, and changes in average Brownian displacement and thermophoresis displacement were checked for atomic behavior. The obtained findings can be useful in different industries to achieve products with optimal thermal capabilities.

## 2. Numerical method

### 2.1. Simulation detail

In this research, the copper channel is first simulated in three directions with periodic boundary conditions, and then the water/graphene NF enters the channel. Fig. 1 shows the schematic and direction of fluid flow. It should be noted that the simulated graphene is in the form of an armchair, as shown in Fig. 1. Then, by using Avogadro and Packmol softwares, the prototype of the structure was prepared, and the desired structure was developed in three directions of the coordinate axes. The copper channel was modeled by LAMMPS software. Fig. 1 depicts a view of the simulated sample. Then, the NPT ensemble and initial conditions (300 K and 1 bar) were imposed. In the next stages, the NPT ensemble was replaced by the NVE ensemble, and thermal behavior and Brownian motion and thermophoresis of water/graphene NF were investigated by reporting temperature profile, HF, TC, Brownian motion, and thermophoresis. For more information about formulation of the problem, please see supporting information (See Appendix A).

## 3. Results

### 3.1. Equilibration process

First, the equilibrium was investigated in the atomic sample, including water/graphene NF and copper channels. Therefore, the initial temperature of the structure was set at  $T=300$  K and the simulation was run for 10 ns with the Nose-Hoover thermostat. Fig. 2 depicts the temperature changes. As can be seen, the temperature in the modeled sample converges to  $T=300$  K after 10 ns. It is clear that as more simulation time passed, the temperature fluctuations decrease, and the value of this quantity reaches to 300 K. This behavior is the result of the reduction of the oscillation amplitude of the atoms with the progress of the simulation, which occurred as a result of the proportionality of the simulated atomic structure and the defined force field.

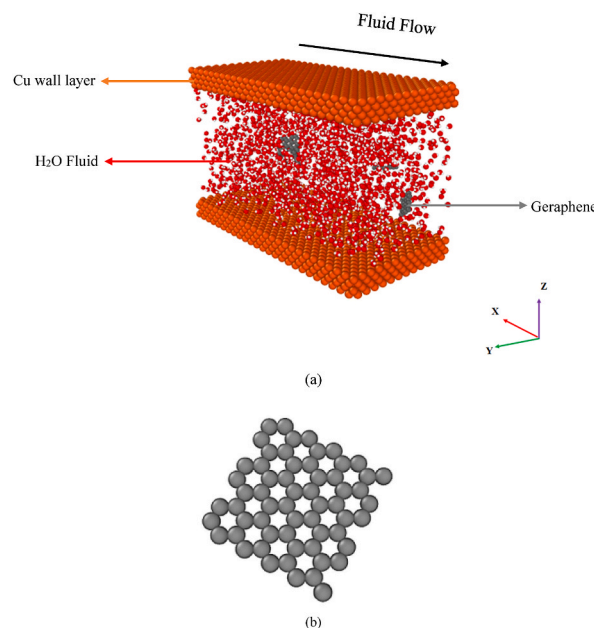


Fig. 1. A view of the a) structure of water/graphene NF and b) graphene structure.

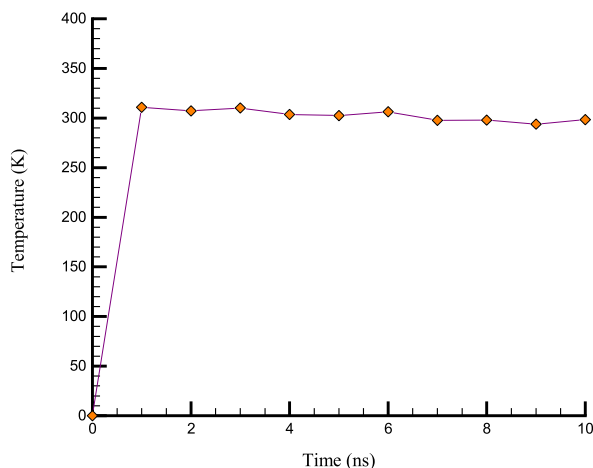


Fig. 2. The temperature changes of the structure after 10 ns.

Fig. 3 shows the changes in kinetic energy in terms of simulation time. Due to the direct relationship between temperature and kinetic energy, changes in kinetic energy in the atomic sample with respect to time also display the similar results. In other words, as more simulation time passes, the kinetic energy converges to 430 eV. This behavior was the result of the decrease in the mobility of the atomic sample over time and indicates the lack of increase in the structural disorder within the defined channel. This convergence in kinetic energy and temperature resulted from proper simulation settings, which is considered a kind of validation of the present calculation method.

After observing the balance in the structure, the calculation method was validated. For this purpose, the radial distribution function (RDF) between oxygen-oxygen in water molecules in the defined aqueous medium was calculated and reported. The obtained results for this quantity are presented in Fig. 4. In this part, the RDF of  $O_2$  was calculated to validate the results of MD simulations. Physically, the RDF in an atomic structure represents particles' relative arrangement. Calculating the RDF was a compelling way to recognize between different atomic structures, agreeing with the basic concepts of the MD simulation. The atomic neighbors of the core atom are represented by the peaks formed in the RDF of an atomic sample from a physical perspective. As a result, this function had a distinct peak for various gas-phase structures, after which its numerical value tended to be constant.

On the other hand, the RDF for atomic structures in the liquid phase shows a clear peak and multiple subsidiary peaks. Similar peaks of approximately equal size were expected for RDF of solid structures. The pattern of this RDF was not changed over time in atomic samples, and consequently, it could be compared with previous results. Comparing this quantity shows an acceptable correspondence between the simulations performed and previous studies [35,36], which shows the scientific validity of the results obtained from MD simulations. Based on the diagram, the initial peak was occurred after 10 ns near the 2.5 Å point.

### 3.2. The atomic wall layers

Changes in the initial conditions of atomic structures can directly affect their performance. One of the ways to change the HF in the designed structures is to change the thickness of the atomic channel walls. At this stage, the process described with the number of

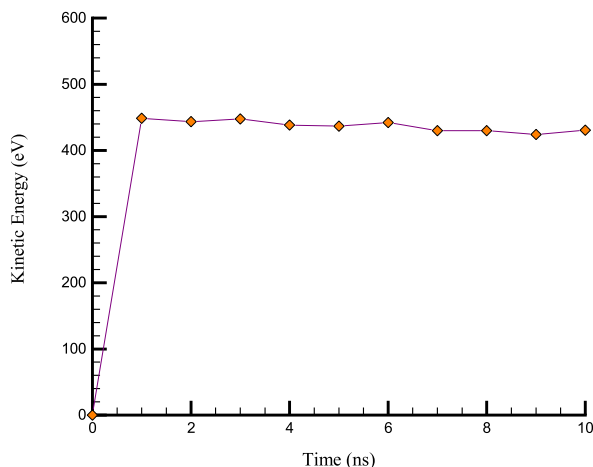


Fig. 3. The changes in kinetic energy of the structure versus simulation time at the initial temperature of 300 K.

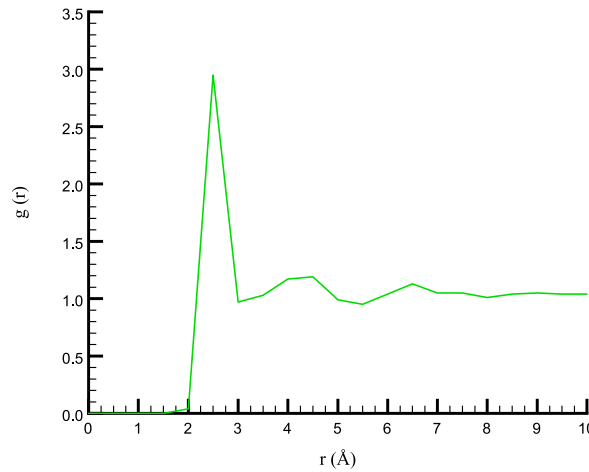


Fig. 4. RDF of oxygen-oxygen in water molecules at an initial temperature of 300 K.

atomic layers of the channel wall) 4, 5, 6, and 7 (was investigated. Fig. 5 depicts the changes in average Brownian displacement versus the number of atomic layers after 10 ns. In line with the mentioned diagram, by raising the layers from 4 layers to 7 layers, the average Brownian displacement rose from 3.06 to 3.62 Å. As the number of layers of the structure increases, the temperature decreases. This decrease in temperature causes a more significant temperature difference between the hot and cold areas. A more significant temperature difference causes the movement of more molecules. As a result, by increasing the number of layers, heat transfer is done faster and better. Finally, the number of layers increases the average atomic displacements, and the average Brownian displacement of the final sample increases significantly.

Fig. 6 displays the changes in the average displacement of thermophoresis versus the number of atomic layers after 10 ns. Thermophoresis is a phenomenon observed when a mixture of two or more moving particles is subjected to the force of a temperature gradient. This phenomenon is essential in the free movement process, where the flow is based on buoyancy force and temperature. Particles move in the direction of decreasing temperature. Due to the effect of temperature gradient on the displacement of thermophoresis, with the increase of atomic layers and the subsequent increase in the movement of atoms, the temperature gradient increases along the channel in the flow direction. As a result, due to the rise of the temperature gradient, the displacement of thermophoresis increases. Finally, increasing the atomic channel wall layers increases the average thermophoresis displacement. Apparently, by raising the layers from 4 layers to 7 layers, the average thermophoresis displacement rises from 23.88 to 25.05 Å. In other words, by raising the number of atomic layers, the design structure is done, the temperature increase created in the cold area is increased for the hot area, and finally, this process causes more mobility of the simulated atoms and optimal heat transfer inside the simulated atomic channel. Finally, increasing the number of atomic channel wall layers increases the average thermophoresis displacement.

Increasing the intensity of NF particle transfer for atomic channel walls with more layers made thermal energy transfer more intensively into the designed structure. This physical claim can be evaluated by examining the HF transferred inside the atomic

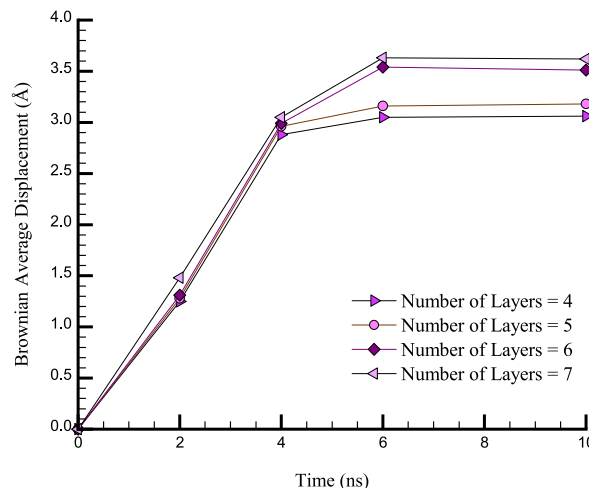


Fig. 5. Changes in Brownian average displacement versus atomic wall layers after 10 ns.

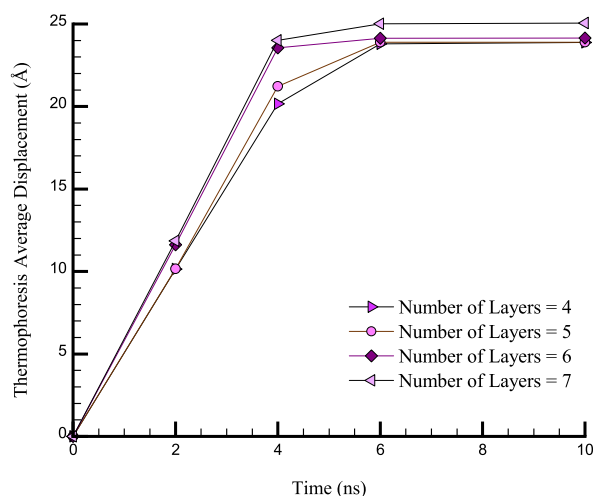


Fig. 6. Changes in average thermophoresis displacement versus the atomic wall layers after 10 ns.

channel. For this purpose, calculations related to the HF inside the simulation box were performed, and the results are presented in Fig. 7. Numerically, by raising the number of atomic layers of the channel wall, the HF increases from  $39.54 \text{ W/m}^2$  to  $41.18 \text{ W/m}^2$  after 10 ns. This process was due to the expansion of the hot areas inside the channel by increasing the number of atomic layers of the wall of a microchannel, which led to an increase in thermal conductivity (TC) of the entire atomic structure.

Fig. 8 shows the TC of the structure with increasing atomic layers. It is clear that by raising the atomic layers from 4 to 7, the TC increases from  $0.36 \text{ W/mK}$  to  $0.42 \text{ W/mK}$ . The increase in atomic layers, atomic fluctuations, average Brownian displacement, and thermophoresis increase the heat transfer rate.

Fig. 9 depicts the temperature profile in the atomic channel according to the number of layers of the atomic channel. The results indicate the maximum temperature value at the maximum distance from the channel walls. In other words, by increasing the number of atomic layers from 4 layers to 7 layers, the maximum temperature increases from  $1415 \text{ K}$  to  $1538 \text{ K}$  and improves the temperature profile. In the fully developed region, the diffusion due to thermophoresis is greater than the diffusion due to the Brownian motion of the nanoparticles. Hence, the accumulation of nanoparticles in the central regions of the channel is higher. However, a more uniform distribution of nanoparticles is observed in the entrance area. As a result, the peak can be seen in the middle of the channel. At the peak, the maximum temperature increases as the number of layers increases.

All numerical results obtained are presented in Table 1. The existence of equilibrium in this stage of simulations and the non-destruction of the atomic structure of the simulated NF guaranteed the use of defined atomic samples in laboratory conditions. To ensure the existence of balance in the atomic structures, the composition of these samples from a close-up view and in different numbers of layers is presented in Fig. 10.

#### 4. Conclusion

Since the increase of heat transfer is always required for modern industrial applications, conventional methods alone are not the answer, and the methods of increasing heat transfer are of serious interest to researchers in this regard. One of the new methods is the use of NFs. The movement of nanoparticles in base fluids is caused by seven sliding mechanisms: inertia, Brownian motion, thermophoresis, Magnes effects, gravity effect, diaphoresis effect, and fluid discharge effect. Of the above seven mechanisms, only Brownian motion and thermophoresis are necessary for the sliding mechanism in NF. As a result, in this research, the Brownian motion, and thermal behavior of water/graphene NF affected by the atomic wall layers (4, 5, 6 and 7) were studied using MD method. To conduct this investigation, the designed NF was first simulated inside a copper nanochannel and then was evaluated in equilibrium and structural/thermal transformation. The most eminent results are listed as follows:

- With the passing of the simulation time in the defined atomic sample, the atomic oscillations inside the simulation box decrease, and the values of kinetic energy and temperature in the final sample converge to  $430 \text{ eV}$  and  $300 \text{ K}$ , respectively.
- Increasing the number of layers due to the decrease in temperature increases the temperature difference between the hot and cold points along the channel. It improves the Brownian motion and the maximum temperature.
- Raising the atomic layers from 4 to 7 increases the average Brownian displacement and thermophoresis displacement from  $3.06 \text{ \AA}$  and  $23.88 \text{ \AA}$  to  $3.62$  and  $25.05 \text{ \AA}$ , respectively.
- Raising the channel wall's atomic layers increases the HF and TC values from  $39.54 \text{ W/m}^2$  and  $0.36 \text{ W/mK}$  to  $41.18 \text{ W/m}^2$  and  $0.42 \text{ W/mK}$  after 10 ns, respectively.
- By rising the number of atomic layers, from 4 to 7, the maximum temperature rose from  $1415 \text{ K}$  to  $1538 \text{ K}$ .
- Increasing the atomic layers of the wall improves the thermal behavior of the structure.

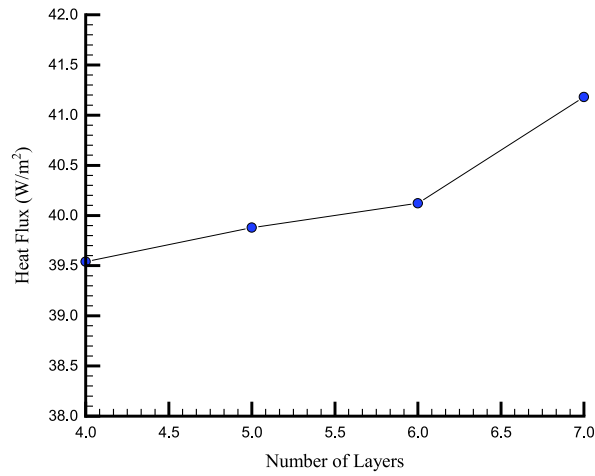


Fig. 7. HF changes in the structure versus the atomic wall layers after 10 ns.

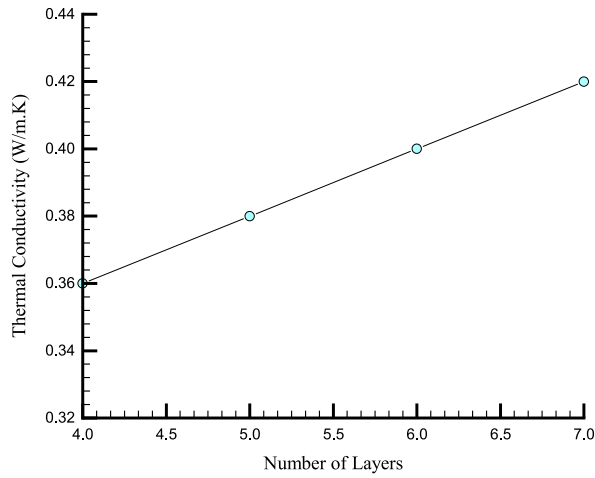


Fig. 8. Variations of the TC in the structure in terms of the atomic wall layers after 10 ns.

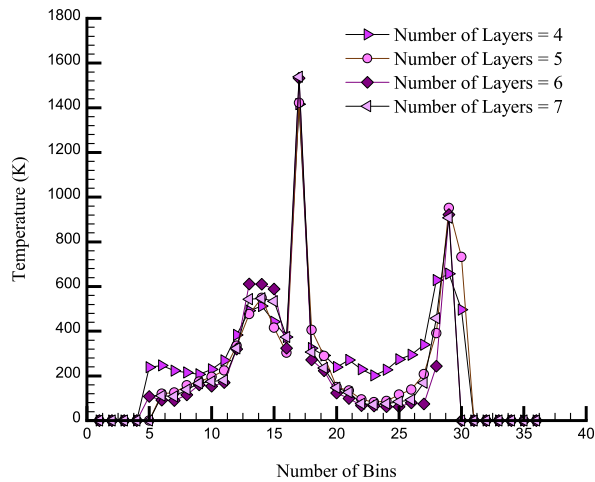
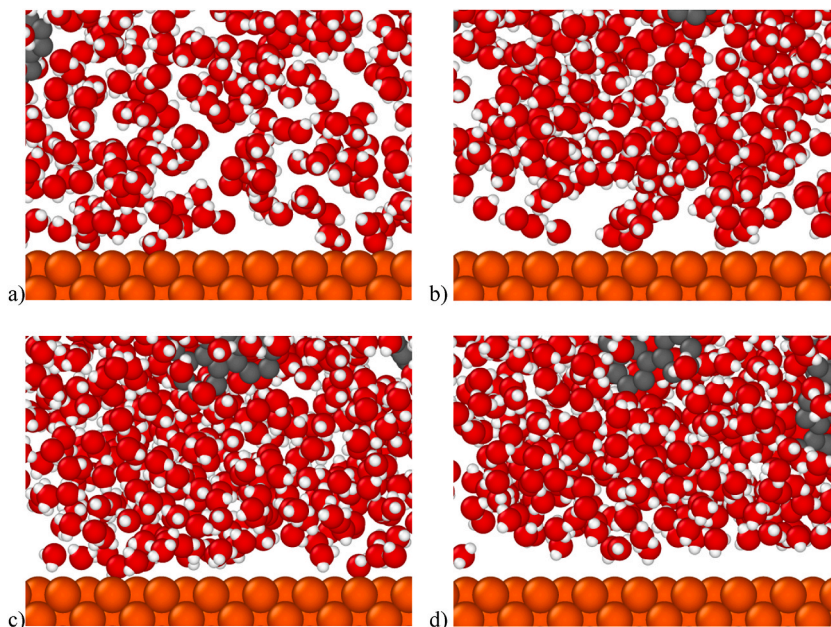


Fig. 9. Temperature profile in structure versus the atomic wall layers after 10 ns.

**Table 1**

Changes in average Brownian displacement, average thermophoresis displacement, HF, TC, and maximum temperature in the structure after 10 ns versus the number of atomic wall layers.

Atomic wall layers	Brownian displacement (Å)	Thermophoresis displacement (Å)	HF (W/m <sup>2</sup> )	TC (W/m.K)	Maximum temperature (K)
4	3.06	23.88	39.54	0.36	1415
5	3.18	23.90	39.88	0.38	1421
6	2.51	24.15	40.12	0.40	1532
7	2.62	25.05	41.18	0.42	1538



**Fig. 10.** The atomic structure defined in the present research in the final stage of MD at atomic wall layers a) 4, b) 5, c) 6, and d) 7 layers.

#### Author statement

- The corresponding author is responsible for ensuring that the descriptions are accurate and agreed by all authors.
- The role(s) of all authors are listed.
- Authors have contributed in multiple roles.

**Methodology, Software and Validation:** Xinwei Guo, Dheyaa J. Jasim, As'ad Alizadeh, Navid Nasajpour-Esfahan, Soheil Salahshour, Mahmoud Shamsborhan, Rozbeh Sabetvand, **Writing - Original Draft:** Dheyaa J. Jasim, As'ad Alizadeh, Navid Nasajpour-Esfahan, Mahmoud Shamsborhan, Rozbeh Sabetvand, **\*Investigation:** Dheyaa J. Jasim, As'ad Alizadeh, Babak Keivani, Soheil Salahshour, Rozbeh Sabetvand, **Revision:** Xinwei Guo, Dheyaa J. Jasim, Babak Keivani, Navid Nasajpour-Esfahan, Soheil Salahshour.

#### Declaration of competing interest

The authors declare that they have no known competing financial interests or personal relationships that could have appeared to influence the work reported in this paper.

#### Data availability

No data was used for the research described in the article.

#### Acknowledgment

National Foreign Experts Program (G2023026002L).  
Henan Province Key R&D and Promotion Special Project (232102320206).  
Scientific Research and Development Project of Henan Provincial Department of Housing and Urban-Rural Development (HNJS-2022-K55).

Humanities and Social Sciences Research Project of Universities in Henan Province (2024 -ZDJH-282).

Xi'an University of Science and Technology, State Key Laboratory of Green and Low-carbon Development of Tar-rich Coal in Western China (SKLCRKF22-03).

## Appendix A

### A-1. MD simulation

Computer simulation is one of the greatest methods for examining materials' structure and behavior. MD is one of them; it is a multidisciplinary approach that investigates the connections between molecule structure, motion, and functions. In MD simulation, atoms and molecules may interact for a predetermined amount of time while following the accepted principles of physics, providing insight into particle motion. The basis of MD simulation lies in solving Newton's equations of motion [26,27].

$$F_i = m_i a_i = -\nabla_i U = -\frac{dU}{dr_i} \quad (\text{a-1})$$

In this simulation, the velocity Verlet algorithm can be used as an efficient method for integrating the equations of motion of the algorithm [28,29].

$$r_i(t + \Delta t) = 2r_i(t) - r_i(t - \Delta t) + \left(\frac{d^2 r_i}{dt^2}\right) (\Delta t)^2 \quad (\text{a-2})$$

$$v(t + \Delta t) = v(t) + \Delta t v(t) + \frac{\Delta t (a(t) + a(t + \Delta t))}{2} \quad (\text{a-3})$$

The functional form and its parameters must be specified to define a force field. The non-bonded potential function occurs due to particles in space and has different types [30]. Tersoff, Lennard-Jones, EAM, and Coulomb's potentials were used in this article. In MD simulation, an essential concept is introduced: the concept of total energy in the system. Total energy, denoted as total energy, assumes a pivotal role in MD simulations, serving as a comprehensive measure encompassing the cumulative sum of all interactions manifesting within the system. These interactions encompass diverse forces and energy contributions, spanning the gamut from covalent and non-covalent bonds to electrostatic and van der Waals forces. Consequently, calculating total energy necessitates meticulously considering all these intricate interactions that collectively govern the system's behavior. For clarity and precision, the governing equation encapsulating this fundamental concept is presented [27].

$$E_{total} = E_{bonded} + E_{nonbonded} \quad (\text{a-4})$$

In MD simulation, the direct computation of forces emanating from an infinite multitude of particles constitutes a formidable and exceedingly time-consuming challenge. Given the impracticality of resorting to qualitative methods, resolving these complex computational challenges necessitates the judicious utilization of mathematical functions and potential models. Within the context of this research, the intricate dynamics of particle interactions are mathematically modeled through the adoption of specific potential functions. In non-bonded interactions, all pairs of particles  $i$  and  $j$ , which are placed at a distance  $r_{ij}$  from each other, interact with each other on the effect of the Lennard-Jones (LJ) potential [31]:

$$U_{LJ} = 4\epsilon_{ij} \left[ \left(\frac{\sigma_{ij}}{r_{ij}}\right)^{12} - \left(\frac{\sigma_{ij}}{r_{ij}}\right)^6 \right] r < r_c \quad (\text{a-5})$$

$\epsilon_{ij}$ ,  $\sigma_{ij}$ , and  $r$  are the depth of particle potential well, the finite distance in which the potential was zero, and the distance among the particles. The Lennard-Jones potential coefficients for the particles present in the upcoming simulation are reported in Table 1.

**Table a-1**  
Lennard-Jones potential parameters of present particles [29,32].

Atom	$\epsilon_{ij}$ (kcal/mol)	$\sigma_{ij}$ (Å)
C	0.105	3.851
H	0.044	2.886
O	0.060	3.500
CU	0.005	3.495

EAM potential is used to simulate the interplays of metal systems. Johnson and Dow first introduced this potential in 1988 and 1989. One of the features of this potential is the ability to describe bonds that deal with certain complexities. This complexity in this type of system is the creation of bonds when the metal atom is placed in the electron cloud of the host atom. Such interactions are described as an experimental function of submerged energy. This function describes interactions by considering many binary and polyatomic effects. The total energy of such a system is written as Eq.a-6 [33]:

$$U_{\alpha\beta} = G_{\alpha} \left( \sum_{j \neq i} \rho_j^{\beta} (r_{ij}) \right) + \frac{1}{2} \sum_{j \neq i} \phi_{\alpha\beta} (r_{ij}) \quad (\text{a-6})$$

Based on the above equation, the potential is defined as the energy required to place atom  $i$  in the superelectronic space of atom  $j$ .  $G_{\alpha}$  is the latent energy or force of the  $i$  atom (type  $\alpha$ ) in the electron space of other atoms.  $U_{\alpha\beta}$  is a function of the interatomic potential,  $\rho_j^{\beta}$  is the average electron density of the host atom  $j$ , and  $r_{ij}$  is the interval between the atoms  $i$  and  $j$ .

The attraction potential is a three-particle potential and is very suitable for simulating atoms bound together by covalent bonds. This potential is a very good approximation for simulating carbon structures such as graphene sheets, carbon tubes, porous carbon, etc. [34]:

$$E = \frac{1}{2} \sum_i \sum_{j \neq i} V_{ij} \quad (\text{a-7})$$

Finally, electric potential energy is obtained from Coulomb's constant forces. This energy determines the force of static electric charges of the particles of a system that repel or attract each other [34]:

$$U_{ij}(r) = \frac{-1}{4\pi\epsilon_0} \frac{q_i q_j}{r_{ij}^2} \quad (\text{a-8})$$

## References

- [1] R. Saidur, K. Leong, H.A. Mohammed, A review on applications and challenges of nanofluids, *Renew. Sustain. Energy Rev.* 15 (3) (2011) 1646–1668.
- [2] S.K. Das, S.U. Choi, W. Yu, T. Pradeep, *Nanofluids: Science and Technology*, John Wiley & Sons, 2007.
- [3] V. Dubey, A.K. Sharma, A short review on hybrid nanofluids in machining processes, *Adv. Mater. Proces. Technol.* 9 (1) (2023) 138–151.
- [4] M. Li, B. Yin, C. Gao, J. Guo, C. Zhao, C. Jia, X. Guo, Graphene: Preparation, Tailoring, and Modification, 2023, pp. p20–p25.
- [5] M. Bahiraei, S. Heshmatian, Graphene family nanofluids: a critical review and future research directions, *Energy Convers. Manag.* 196 (2019) 1222–1256.
- [6] F. Sultan, W. Khan, M. Ali, M. Shahzad, M. Irfan, M. Khan, Theoretical aspects of thermophoresis and Brownian motion for three-dimensional flow of the cross fluid with activation energy, *Pramana* 92 (2019) 1–10.
- [7] N. Bou-Rabee, M.C. Holmes-Cerfon, Sticky Brownian motion and its numerical solution, *SIAM Rev.* 62 (1) (2020) 164–195.
- [8] Y. Zhou, M. Yu, Z. Shi, A Review of Particle Removal Due to Thermophoretic Deposition, 2023.
- [9] M. Sheikholeslami, Z. Shah, A. Shafee, I. Khan, I. Tlili, Uniform magnetic force impact on water based nanofluid thermal behavior in a porous enclosure with ellipse shaped obstacle, *Sci. Rep.* 9 (1) (2019) 1196.
- [10] N. Alilat, E.B. Martin, F. Sastre, J.A. Millán García, A. Bañri, Thermal behavior of a conical antenna cooled with nanofluid saturated porous media: effects of the cavity's inclination and aspect ratio, *Int. J. Numer. Methods Heat Fluid Flow* 32 (12) (2022) 3935–3947.
- [11] A. Chattopadhyay, R. Malo, H.F. Öztop, S.K. Pandit, K.D. Goswami, Simulation of magneto mixed convective flow and thermal behavior of hybrid nanofluid in a partially heated wavy cavity, *J. Magn. Magn. Mater.* 575 (2023), 170713.
- [12] D. Li, C. Jiang, X. Cao, H. Li, M. Hekmatifar, R. Sabetvand, Effect of cross-sectional area and number of Fe nanoparticles on the thermal behavior of pool boiling heat transfer of the water-based nanofluid: a molecular dynamics study, *Case Stud. Therm. Eng.* 36 (2022), 102242.
- [13] B. Ruhani, M.T. Andani, A.M. Abed, N. Sina, G.F. Smaism, S.K. Hadrawi, D. Toghraie, Statistical modeling and investigation of thermal characteristics of a new nanofluid containing cerium oxide powder, *Heliyon* 8 (11) (2022).
- [14] M. Zamen, M. Kahani, B. Rostami, M. Bargahi, Application of Al2O3/water nanofluid as the coolant in a new design of photovoltaic/thermal system: an experimental study, *Energy Sci. Eng.* 10 (11) (2022) 4273–4285.
- [15] S. Akram, M. Athar, K. Saeed, A. Razia, T. Muhammad, Hybridized consequence of thermal and concentration convection on peristaltic transport of magneto Powell–Eyring nanofluids in inclined asymmetric channel, *Math. Methods Appl. Sci.* 46 (10) (2023) 11462–11478.
- [16] Y. Khan, S. Akram, M. Athar, K. Saeed, T. Muhammad, A. Hussain, M. Imran, H. Alsulaimani, The role of double-diffusion convection and induced magnetic field on peristaltic pumping of a Johnson–Segalman nanofluid in a non-uniform channel, *Nanomaterials* 12 (7) (2022) 1051.
- [17] S. Akram, M. Athar, K. Saeed, M. Imran, T. Muhammad, Slip impact on double-diffusion convection of magneto-fourth-grade nanofluids with peristaltic propulsion through inclined asymmetric channel, *J. Therm. Anal. Calorimetry* (2022) 1–14.
- [18] Y. Khan, S. Akram, A. Razia, A. Hussain, H. Alsulaimani, Effects of double diffusive convection and inclined magnetic field on the peristaltic flow of fourth grade nanofluids in a non-uniform channel, *Nanomaterials* 12 (17) (2022) 3037.
- [19] S. Akram, A. Razia, Hybrid effects of thermal and concentration convection on peristaltic flow of fourth grade nanofluids in an inclined tapered channel: applications of double-diffusivity, *CMES-Computer Model. Eng. Sci.* 127 (3) (2021).
- [20] K. Saeed, S. Akram, A. Ahmad, Outcomes of partial slip on double-diffusive convection on peristaltic waves of johnson–segalman nanofluids under the impact of inclined magnetic field, *Arabian J. Sci. Eng.* (2023) 1–17.
- [21] S. Akram, K. Saeed, M. Athar, A. Razia, A. Hussain, I. Naz, Convection theory on thermally radiative peristaltic flow of Prandtl tilted magneto nanofluid in an asymmetric channel with effects of partial slip and viscous dissipation, *Mater. Today Commun.* 35 (2023), 106171.
- [22] S. Akram, M. Athar, K. Saeed, A. Razia, T. Muhammad, Theoretical Investigation of Double Diffusion Convection of Six Constant Jeffreys Nanofluid on Waves of Peristaltic with Induced Magnetic Field: a Bio-Nano-Engineering Model, *Waves in Random and Complex Media*, 2022, pp. 1–21.
- [23] X. Liu, I. Patra, O.R. Kuzichkin, M. Zaidi, S.M. Abdulnabi, Z. Mohsen Najm, U.S. Altimari, S.K. Hadrawi, M. Taheri Andani, M. Hekmatifar, Molecular dynamics study of the effect of external electric field amplitude and cavity on thermal properties of Ammonia/Copper Nano-Refrigerant, *Journal of Molecular Liquids* 365 (202125) (2022) 120125. <https://doi.org/10.1016/j.molliq.2022.120125>.
- [24] X. Liu, B. Ghafari, I. Patra, M.M. Kadhim, A. Turki Jalil, Anil Kumar, R. Sivaraman, N. Nasajpour-Esfahani, M. Taheri Andani, D. Toghraie, A molecular dynamics study of thermal behavior of ammonia/Cu nanorefrigerant flow under different initial pressures and electric fields, *Journal of Molecular Liquids* 367 (20388) (2022) 120388. <https://doi.org/10.1016/j.molliq.2022.120388>.
- [25] S.-R. Yan, N. Shirani, M. Zarringhalam, D. Toghraie, Q. Nguyen, A. Karimipour, Prediction of boiling flow characteristics in rough and smooth microchannels using molecular dynamics simulation: Investigation the effects of boundary wall temperatures, *Journal of Molecular Liquids* 306 (112937) (2020) 112937. <https://doi.org/10.1016/j.molliq.2020.112937>.
- [26] J.D. Bernal, A geometrical approach to the structure of liquids, *Nature* 183 (1959) 141–147.
- [27] D.C. Rapaport, D.C.R. Rapaport, *The Art of Molecular Dynamics Simulation*, Cambridge university press, 2004.
- [28] E. Hairer, C. Lubich, G. Wanner, Geometric numerical integration illustrated by the Störmer–Verlet method, *Acta Numer.* 12 (2003) 399–450.

- [29] A.K. Rappé, C.J. Casewit, K. Colwell, W.A. Goddard III, W.M. Skiff, UFF, a full periodic table force field for molecular mechanics and molecular dynamics simulations, *J. Am. Chem. Soc.* 114 (25) (1992) 10024–10035.
- [30] H.J. Berendsen, J.R. Grigera, T.P. Straatsma, The missing term in effective pair potentials, *J. Phys. Chem.* 91 (24) (1987) 6269–6271.
- [31] D. Toghraie, M. Hekmatifar, Y. Salehipour, M. Afrand, Molecular dynamics simulation of Couette and Poiseuille Water-Copper nanofluid flows in rough and smooth nanochannels with different roughness configurations, *Chem. Phys.* 527 (2019), 110505.
- [32] S.L. Mayo, B.D. Olafson, W.A. Goddard, DREIDING: a generic force field for molecular simulations, *J. Phys. Chem.* 94 (26) (1990) 8897–8909.
- [33] F. Shamsedinov, Z. Zaripov, I.M. Abdulagatov, M.L. Huber, F. Gumerov, F. Gabitov, A.F. Kazakov, Experimental study of the thermal conductivity of ammonia+water refrigerant mixtures at temperatures from 278 K to 356 K and at pressures up to 20 MPa, *Int. J. Refrig.* 36 (4) (2013) 1347–1368.
- [34] P.G. Huray, *Maxwell's Equations*, John Wiley & Sons, 2011.
- [35] D.H. Brookes, T. Head-Gordon, Family of oxygen–oxygen radial distribution functions for water, *J. Phys. Chem. Lett.* 6 (15) (2015) 2938–2943.
- [36] P. Cicu, P. Demontis, S. Spanu, G.B. Suffritti, A. Tilocca, Electric-field-dependent empirical potentials for molecules and crystals: a first application to flexible water molecule adsorbed in zeolites, *J. Chem. Phys.* 112 (19) (2000) 8267–8278.